A Low-Profile Hybrid-Fed Dual-Polarized Antenna with High Isolation and High Cross-Polar Discrimination

M. Ciydem [1] and E. A. Miran [2]

[1] Dept. of Electrical and Electronics Engineering, Faculty of Engineering
Gazi University, 06570 Maltepe, Ankara, Turkey
mehmetciydem@gazi.edu.tr

[2] Dept. of Electrical and Electronics Engineering, Middle East Technical University, 06520 Balgat, Ankara, Turkey
alpmiran@gmail.com

Abstract ─ This work presents a wideband hybrid-fed ±45º linear dual-polarized patch antenna design for sub-6 GHz 5G base stations. Two polarizations are created by a slot-coupling with rectangular H-slot (+45°) and a capacitive coupling with modified L-probe (–45°). Antenna exhibits wideband −10 dB impedance bandwidths of 40.7% and 35.6% for slot-fed and probe-fed ports, respectively. Due to the special design of suspended stacked patches with hybrid-fed excitations, high port isolation (< –47 dB) and high cross-polar discrimination (> 38 dB) are achieved. Symmetric and directional radiation patterns with stable gain are obtained in E and H planes for each polarization. Compared to its bandwidth, antenna is low-profile (10.6 mm) with front-to-back ratio greater than 22 dB. Simulations and experimental results are reported and discussed.

Index Terms ─ 5G base station, cross-polar discrimination, dual-polarization, hybrid feeds, isolation, low-profile, massive MIMO, sub-6 GHz, wideband patch antenna.

I. INTRODUCTION

Dual-polarization (±45° or Vertical/Horizontal (V/H)) is commonly employed in base station antennas since it helps to fight against multipath and increase in capacity by polarization diversity [1-2]. Moreover, today's base station antennas require wide impedance bandwidth (IBW), good matching level ($|S_{11}|$, $|S_{22}| < -15$ dB), high port isolation ($|S_{21}| < -20$ dB), high front to back ratio (FBR > 20 dB), and high cross-polar discrimination (XPD > 15 dB within ± 30° of boresight). Hence it is not easy to meet all these requirements simultaneously in the same design. With the advent of 5G technology, massive multiple-input multiple-output (mMIMO) has been one the key enabling technologies to reach the goals of 5G. High isolation and high XPD are more desirable in mMIMO array than in conventional (2G/3G/4G-LTE) base station antennas to make full use of it, especially for low envelope correlation coefficient (ECC) [3]. In space-limited applications such as mMIMO arrays with huge number of antenna elements, compactness and low-profile of the antenna are also preferable. Therefore, design of a dual-polarized antenna element with high isolation and high XPD satisfying all above requirements facilitates mMIMO array to reach desired performance since it is a building element of that array.

Crossed-dipoles [2,4,5] and patch antennas [5-14] are used in base stations in dual polarization configuration with a pair of feeds. Crossed-dipole antennas are good in terms of wide IBW, high isolation and high XPD. However, they have complex feeding structure with balun and high profile. Moreover, they are not easy to be integrated with planar circuit elements for mMIMO applications. Patch antennas can be preferred in mMIMO arrays owing to their compactness, low-profile, and lightweight. However, they have suffered from narrowband operation, and many efforts on different feeding techniques [5-14] have been developed to improve their performance.

In dual-polarized patch antennas, feeds excite the patch and creates desired fundamental modes and undesired higher order modes. Currents of flowing on the feeds-ground plane whose interactions with patch and with each other are the main factors determining the isolation and XPD. Hence, feeding structures and feed types play an important role in the design. A variety of techniques [3, 15-23] for high isolation and high XPD have been developed for patch antennas. For the same type of feeds (slot-slot, probe-probe), differential feeding [3,15,16], which utilizes 180° phase difference between feeds to suppress higher order modes, helps to improve isolation and XPD. However, differential feeding may bring complexity in feeding network and sometimes difficulty in obtaining wide IBW. Moreover, in slot-slot configuration, an additional reflector plate which increases antenna profile, may be required to reduce back

Submitted On: April 20, 2021
Accepted On: July 25, 2021

https://doi.org/10.47037/2021.ACES.J.360907

radiation of slots for high FBR. But the ground plane and reflector plate may form a waveguide and some modes may propagate inside this causing again deterioration of isolation and XPD. Then hybrid feeds (slot-probe) may be employed as a solution for high isolation and high XPD since probe feed (capacitively coupled) has almost no coupling current on the ground plane and hence coupling and cross polarization between slot-probe will be eliminated on the ground plane. Furthermore, the mechanism for tuning and radiation of hybrid-fed antenna will be totally different for slot-fed and probe-fed ports, and this property may be used as an advantage for high isolation and high XPD. On the other hand, this brings difficulties in achieving separate designs which satisfy all performance requirements for each feed (polarization) utilizing the same radiating patches of hybrid-fed antenna.

In literature, several dual-polarized hybrid-fed patch antenna designs [17-23] have been reported. Two hybrid-fed designs with slot-probe feeds are proposed in [17,18] achieving high isolation and high XPD but they operate in 2.2-2.6 GHz with 14% IBW. [19] presents a circular patch antenna with conical (omni) and broadside modes using hybrid feed network of H-slot and probe feeds. The goal of [19] is to have different characteristics (radiation pattern, gain, S-parameters) in each polarization and to utilize them as multifunction and diversity antennas. However, this is not the case for 5G mMIMO arrays which require similar characteristics and performance for both polarizations in order to achieve low ECC [3]. In [20], a hybrid-fed dual-polarized patch antenna has been introduced but it is very narrow band. Moreover, its isolation and XPD levels are not satisfactory. [21] implements hybrid-fed antenna with a pair of hook shaped probes with 180° phase difference for one polarization and magnetic-coupled metallic loop for the other polarization. Its performance is good in many aspects but does not cover sub-6 GHz 5G spectrum (3.3-3.8 GHz) completely. In [22], a balanced-probe feed and a slot feed is implemented for V/H polarizations for meteorological radar which requires high isolation and high XPD. Another novel hybrid-fed patch antenna with electric-coupled and magnetic coupled feeds has been reported in [23]. Recently, a meta-material based decoupling structure in X-band for high isolation has also been introduced in [24]. Performance summary and comparison of similar works are given in Table 1.

To the best of authors' knowledge, hybrid-fed patch antenna design for sub-6 GHz 5G applications has not been investigated sufficiently yet. Therefore, this study deals with design of a low profile, wideband, dual-polarized hybrid-fed patch antenna with high isolation and high XPD. Although it is intended to operate in 3.3-3.8 GHz, slot feed (port-1) and probe feed (port-2) exhibits much more wider IBW. Proposed antenna provides similar s-parameter performance, gain and broadside radiation patterns in principal planes for both polarizations. The antenna can also be assumed to be low-profile (10.6 mm) with its IBW and operating band when compared to similar works in Table 1.

Table 1: Comparison of related works (NG: Not Given)

Ref.	Antenna and Feed Type	IBW (GHz, %)	Matching $\lvert S_{11}\rvert$, $\lvert S_{22}\rvert$ (dB)	Isolation $\lvert S_{21}\rvert$ (dB)	FBR (dB)	XPD (dB)	Dimensions (mm)
[3]	Crossed dipole- differential feeding	3.23-5.27, 48%	<−10	< −55	>22	>35	90x90x19.5
[15]	Patch-differential feeding	1.84-2.73, 38.7%	<−10	<−40	>12	>24	105x105x19.6
[16]	Patch-differential feeding	3.16-3.74, 17.2%	<−10	<−38.5	>18	>33	80x80x5.8
[17]	Patch-hybrid fed (slot/probe coupled)	1.64-1.88, 13.6% 1.57-2.02, 25%	<−10	<−32	NG	>27	100x100x14.4
[18]	Patch-hybrid feeding (slot/probe coupled)	2.27-2.62, 14.2% 2.24-2.6, 14.5%	<−10	<−40	>12	>35	150x150x13.1
[19]	Patch-hybrid feeding (slot/probe coupled)	2.16-2.72, 23% 2.14-2.64, 20.5%	<−10	<−40	>12	>21	100x100x10.5
[20]	Patch-hybrid feeding (slot/probe coupled)	2.36-2.38, 0.94% 2.35-2.38, 1.33%	<−15	<−24	>15	>15	80x80x1.5
[21]	Patch-hybrid feeding (probe/magnetic coupled)	2.45-3.7, 40.7% 2.6-3.85, 38.7%	<−10	<−40	>20	>30	100x100x17
[22]	Patch-hybrid feeding (slot/probe coupled)	2.58-2.91, 12% 2.51-2.9, 14.4%	<−10	<−43	>25	>32	60x60x7.8
[23]	Patch-hybrid feeding (electric/magnetic coupled)	1.63-2.78, 52% 1.68-2.72, 47.3%	<−10	<−26.5	>16	>23	170x170x25.3
Pro.	Patch-hybrid feeding (slot/probe coupled)	2.95-4.46, 40.7% 3.2-4.59, 35.6%	<−10	<−47	>22	>38	110x110x10.6

II. ANTENNA DESIGN

A. Geometry and configuration

Figure 1 displays structure of the proposed antenna while Table 2 provides its physical parameters and dimensions. The antenna is comprised of a feedline substrate and two square patches (main and parasitic patch), all separated by air. Suspended stacked patches are adopted to have wide IBW. Dual-polarization (±45º) is implemented in hybrid configuration by a slot feed (port-1) and a probe feed (port-2) as shown in Figs. 1-3. Capacitive coupling is realized by a modified L-probe and slot coupling is carried out by a rectangular H-slot. Substrate for the feedline is FR4 (ε_r = 4.4, tanδ = 0.02, h = 1.6 mm). The patches are copper sheets of 0.25 mm thick whose lengths are denoted as L_{p1} and L_{p2}. They are suspended over the feedline substrate at heights of h_{p1} and h_{p2}. The bottom of the feedline substrate contains feeding network for slot feed (port-1) and a ground pad for port-2 while probe feed (port-2) resides on its topside together with the H-slot etched on the common ground. The ground pad and the common ground are connected by four conducting posts so that outer conductor of SMA connector touches the ground plane. Air gaps are realized using separators of appropriate heights. Finally, the feedline substrate and the patches are assembled by plastic screws. The feeding network of port-1 (+45°) is depicted in Fig. 2. It consists of two parts: (i) matching section and (ii) branch lines. The slot is excited by two parallel 100 Ω microstrip branches separated by a distance of L_d. L-shaped stubs are used to terminate the branches and compensate the reactive part of the input impedance of the patch. A T-junction connects the branches to the matching section which provides wideband matching between the patch and port-1. It includes a two-section binomial transformer. Length of the sections are approximately $\lambda_g/4$ (L_{t1}, L_{t2}) at the center frequency of the intended band, f_c = 3.55 GHz (λ_c = 84.55 mm, $\lambda_g = \lambda_c/\sqrt{\varepsilon_r} \approx 40.31$ mm) where λ_g is guided wavelength. As for port-2 (–45°), a 50 Ω coplanar feed line of length L_{mp} is connected to the modified L-probe whose topside is triangular as shown in Fig. 3.

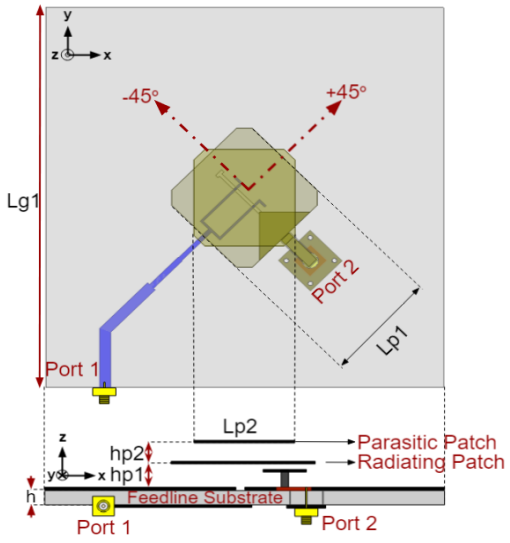

Fig. 1. Antenna configuration and geometry.

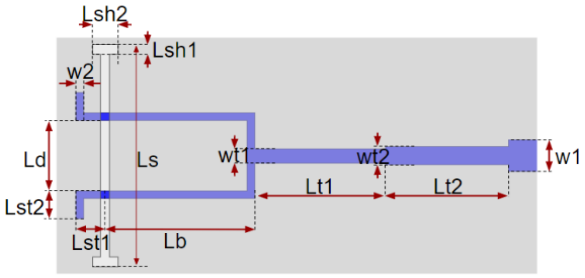

Fig. 2. Feedline and slot-coupled feed (port-1).

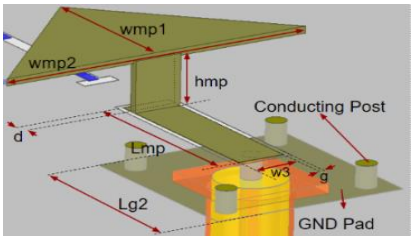

Fig. 3. Capacitively coupled probe feed (port-2).

Table 2: Physical dimensions of the proposed antenna

Description	Parameter	Dimensions (mm)
Ground plane (square) / ground pad (square)	L_{g1} / L_{g2}	110 / 12.4
Main patch (square) / parasitic patch (square)	L_{p1} / L_{p2}	32.5 / 28
Lower/upper air height	h_p /h_{p2}	5 / 4
Slot dimensions / vertical slot width	L_s, L_{sh1}, L_{sh2} / L_{sl2}	20.4, 0.9, 2.3 / 3.2
1st and 2nd binomial section length/width	L_{t1}, L_{t2}, w_{t1}, w_{t2}	11.78, 11.08, 1.32, 1.65
Branch lines separation / branch line length, width	L_d / L_b, w_2	6.53 / 15.48, 0.67
50 Ω line width / co-planar feedline width, length, gap	w_1 / w_3, L_{mp}, g	2.94 / 3, 10.75, 0.35
Probe height / probe offset / probe head	h_{mp} / d / w_{mp1}, w_{mp2}	3.75/ 1 / 10, 20

B. Working principles

Electromagnetic power is coupled to patches through slot and probe, and ±45° dual polarizations are created. Dimensions and placement of the patches at proper heights are of critical importance for good wideband matching, isolation, and FBR. Although the main patch has dominant effect in total design, parasitic one must also be considered in combination with it. The lower h_{p1} makes efficient coupling from slot to the patch easier, hence resulting in good FBR. However, this lower h_{p1} makes broadband operation difficult. On the other hand, the higher h_{p1} facilitates broadband operation but efficient coupling from slot to the patch becomes more difficult and hence resulting in poor FBR. After setting the design of slot feed (port-1) as explained above, the probe feed (port-2), which capacitively couples the energy to the patch, is designed with proper placement of the probe (L_{mp}, h_{mp}). The parasitic patch provides further tuning for each port simultaneously. Existence of the parasitic patch also modifies the current distribution on the main patch, and vectorial combination of currents flowing on the two patches has a total effect of improving the isolation and XPD. Although parasitic patch partially increases the overall antenna profile, it is necessary for design since desired technical performances cannot be obtained by only main patch. However, one can still keep the antenna low-profile.

Figure 4 plots current distributions on the patches, as the antenna is excited from port-1 and port-2 separately, at lower and higher frequency limits of 3.3-3.8 GHz band. When excited from port-1 (Figs. 4 (a)-(b)), currents are established symmetrically around −45° diagonal line on the patches. At 3.3 GHz, amplitude of currents on the main patch gradually increases towards radiating edges, whereas the currents on the parasitic patch are weaker and possess uniform distribution. At 3.8 GHz, stronger coupling is observed between two patches; thus, amplitude of the currents flowing on the parasitic patch increases. This phenomenon leads to resonant behavior around 3.8 GHz. Note that a small portion of the slot is beneath the modified L-shaped probe and this slightly disturbs the current distribution. However, it does not affect the symmetry of the radiation patterns in principal planes as shown later in Fig. 12. Similarly, when excited from port-2 (Figs. 4 (c)-(d)), currents are established symmetrically around +45° diagonal line on the patches. And the antenna again demonstrates its resonant behavior through the parasitic patch at 3.8 GHz. The symmetric characteristics of each polarization along ±45º diagonal line and different distributions of currents (high amplitudes of port-1 and low amplitudes of port-2) for each port reduces the coupling between ports and hence they provide high isolation and high XPD. Moreover, Fig. 5 illustrates simulations of electric field radiated by the slot and coupled to the main patch and the probe. It can be observed that most of the electric field is coupled to the main patch while it is very weak on the probe. This shows that interaction of feeds themselves are reduced by hybrid feeds and it also helps high isolation and high XPD.

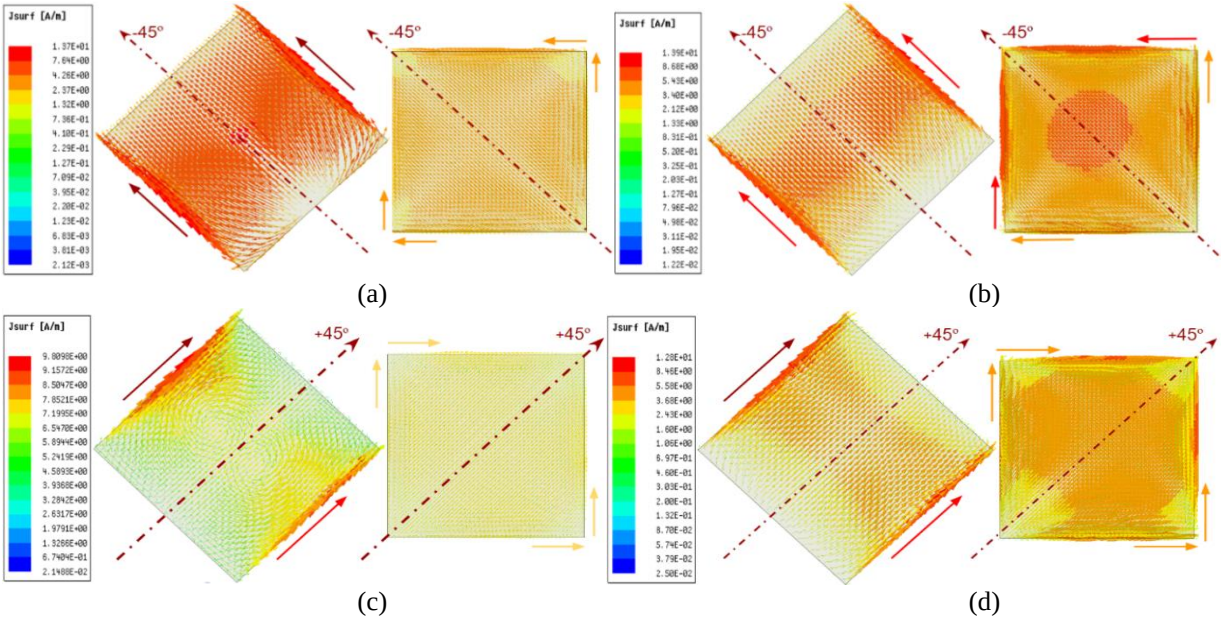

Fig. 4. Current distributions on the patches when the antenna is excited from port-1 at (a) 3.3 GHz and (b) 3.8 GHz; from port-2 at (c) 3.3 GHz and (d) 3.8 GHz.

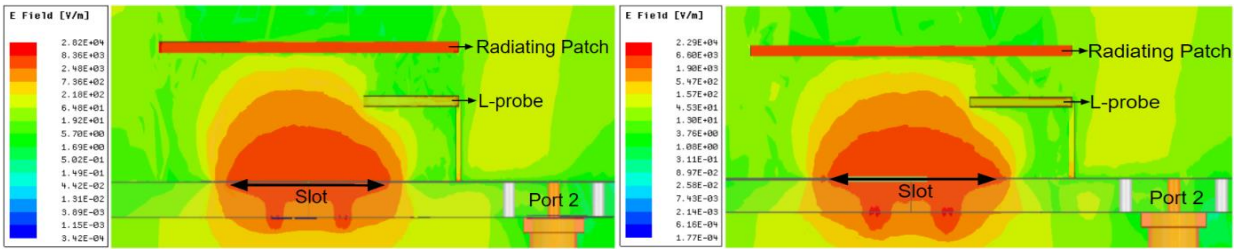

(a) (b)

Fig. 5. E-field distribution when the antenna is excited from port-1 (a) 3.3 GHz and (b) 3.8 GHz.

III. NUMERICAL STUDIES

The proposed antenna is modeled in Ansoft HFSS. A two-stage parametric calculation is carried out in order to obtain optimum electrical performance. In the first stage, slot feed (port-1) is optimized for wideband matching. Then in the second stage, probe feed (port-2) is tuned to give the best matching while checking the isolation performance between the ports. Parametric calculations have been done by sweeping one parameter at a time within a specified range, while keeping the rest unchanged.

A. Slot feed (Port-1)

Owing to simple structure, effect of only one parameter regarding slot feed is reported here. Despite the fact that many other physical aspects (e.g., slot length, stub length, etc.) are also analyzed, they either have minor effects on the antenna performance or none. Patch heights (h_{p1} and h_{p2}) significantly affect wideband matching at port-1. Figure 6 plots $|S_{11}|$ as a function of h_{p1} while it is swept within 4 mm – 6 mm range by 1 mm step. As it is shown, although the IBW is almost the same for all values, h_{p1} = 5 mm yields $|S_{11}| < -18$ dB along 3.3-3.8 GHz band, which is better than the others. After fixing h_{p1} at 5 mm, h_{p2} is swept from 3 mm to 5 mm by 1 mm step and their effects are depicted in Fig. 7. The antenna has its largest −15 dB IBW when h_{p2} = 3 mm and exhibits the best impedance matching level in 3.3-3.8 GHz band when h_{p2} = 5 mm. Here, we decide to select intermediate value of h_{p2} = 4 mm, since it results better matching than h_{p2} = 3 mm and still wide enough IBW although it is less than that of h_{p2} = 5 mm.

B. Probe feed (Port-2)

After the patch heights are fixed for port-1, tuning of the probe feed (port-2) is mainly realized by adjusting the height of the modified L-probe, h_{mp}. Figure 8 illustrates how h_{mp} affects wideband mathcing at port-2. As can be seen, the antenna attains the best impedance matching when h_{mp} = 3.75 mm, i.e., $|S_{22}| < -21$ dB in 3.3-3.8 GHz band and it has wide enough IBW.

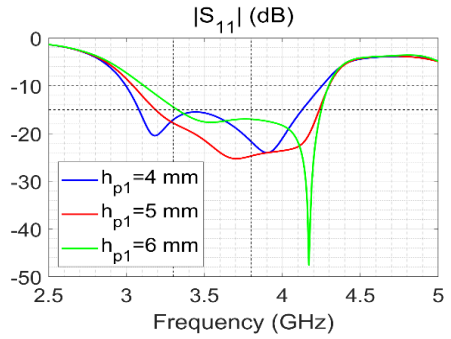

Fig. 6. $|S_{11}|$ as a function of h_{p1} (port-1).

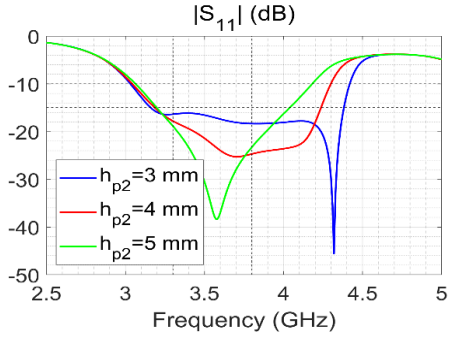

Fig. 7. $|S_{11}|$ as a function of h_{p2} (port-1).

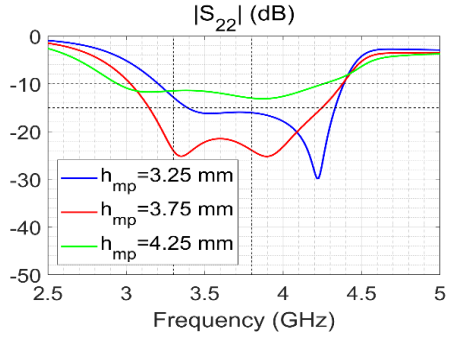

Fig. 8. $|S_{22}|$ as a function of h_{mp} (port-2).

C. Isolation

Finally, with the incorporation of the both feeds described and fixed above, the isolation performance between the ports ($|S_{21}|$) has been checked and obtained to be below −47 dB as shown in Fig. 9. However, it is less than −50 dB in the desired intended band (3.3-3.8 GHz).

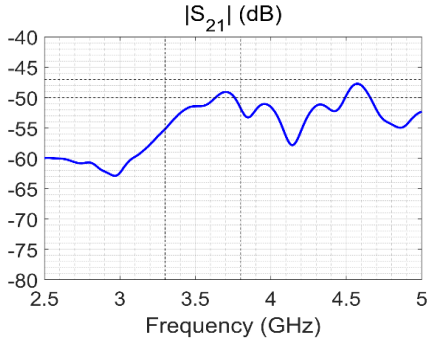

Fig. 9. Simulated port isolation of the antenna.

IV. MEASUREMENT RESULTS

The proposed antenna is prototyped (Fig. 10), in accordance with design descriptions given in Section 2 with FR4 (ε_r = 4.4, tanδ = 0.02) of height 1.6 mm. Galvanized metal sheets of 0.25 mm thickness are used for patches. The overall size of the antenna is 110 mm × 110 mm × 10.6 mm with profile being 10.6 mm.

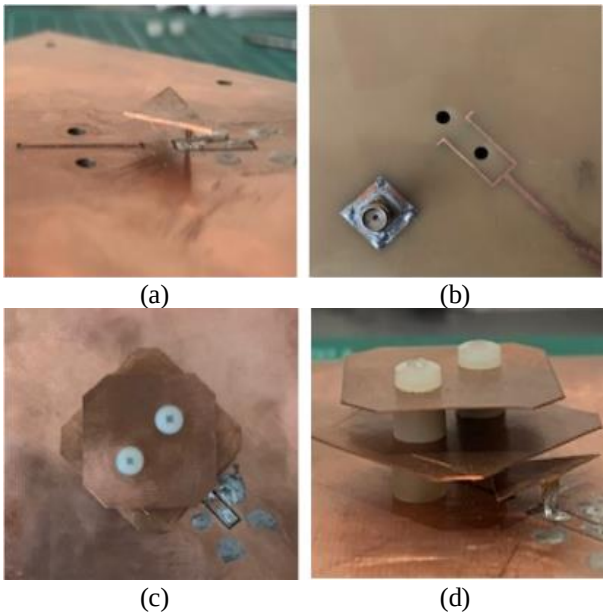

Fig. 10. Prototype antenna (a) slot-probe feeds, (b) feedline layer for slot and SMA connector for probe, (c) top view, and (d) side view.

To prove the proposed design, S-parameters ($|S_{11}|$, $|S_{22}|$, and $|S_{21}|$) and radiation patterns (co-pol and cross-pol) have been measured. S-parameters of the antenna are measured by HP-8720D vector network analyzer and results are given in Fig. 11 in parallel with simulations. The lower and higher limits of the intended operating band (3.3 GHz and 3.8 GHz) are indicated by vertical dashed lines. It must be noted that the discrepancies between them are mostly caused by imperfect assembly and soldering of the components, especially for the modified L-probe (port-2). As shown in Fig. 11, slot feed (port-1) exhibits 40.7% IBW for $|S_{11}| < -10$ dB whereas probe feed (port-2) exhibits 35.6% IBW for $|S_{22}| < -10$ dB. The isolation ($|S_{21}|$) between the ports is less than −47 dB. However, in the operating band (3.3-3.8 GHz), $|S_{11}|$ and $|S_{22}|$ are < −15 dB and $|S_{21}|$ is < −50 dB.

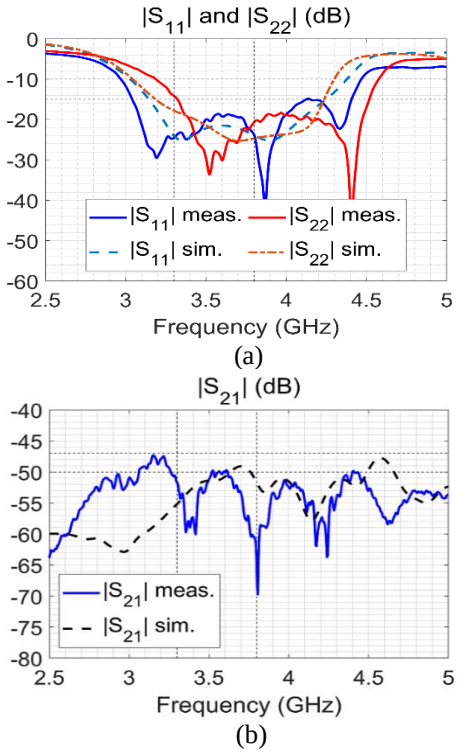

Fig. 11. S-parameters (a) $|S_{11}|$, $|S_{22}|$, and (b) $|S_{21}|$.

The normalized radiation patterns have been measured at 3.3 GHz and 3.8 GHz for both polarizations and plotted in Fig. 12 together with simulations. They are symmetric and directional in broadside. Half power beamwidths (HPBWs) are 50º-60º and 57º-62º for port-1 while they are 56º-64º and 59º-62º for port-2 in E and H planes, respectively. Gain of the antenna varies in 8.5-9.0 dBi for port-1 and in 8.0-8.6 dBi for port-2 as shown in Fig. 13. From radiation patterns, it can also be inferred that XPD levels are greater than 38 dB and 40.5 dB for port-1 and for port-2 respectively, which are measured withing ±30° of boresight. That means a very high XPD has been achieved between two polarizations. High

isolation and high XPD performance are due to very low coupling between the feeds and the patches as explained in Section II-B. In addition, a good FBR is also obtained as 22 dB and 25 dB for port-1 and for port-2 respectively.

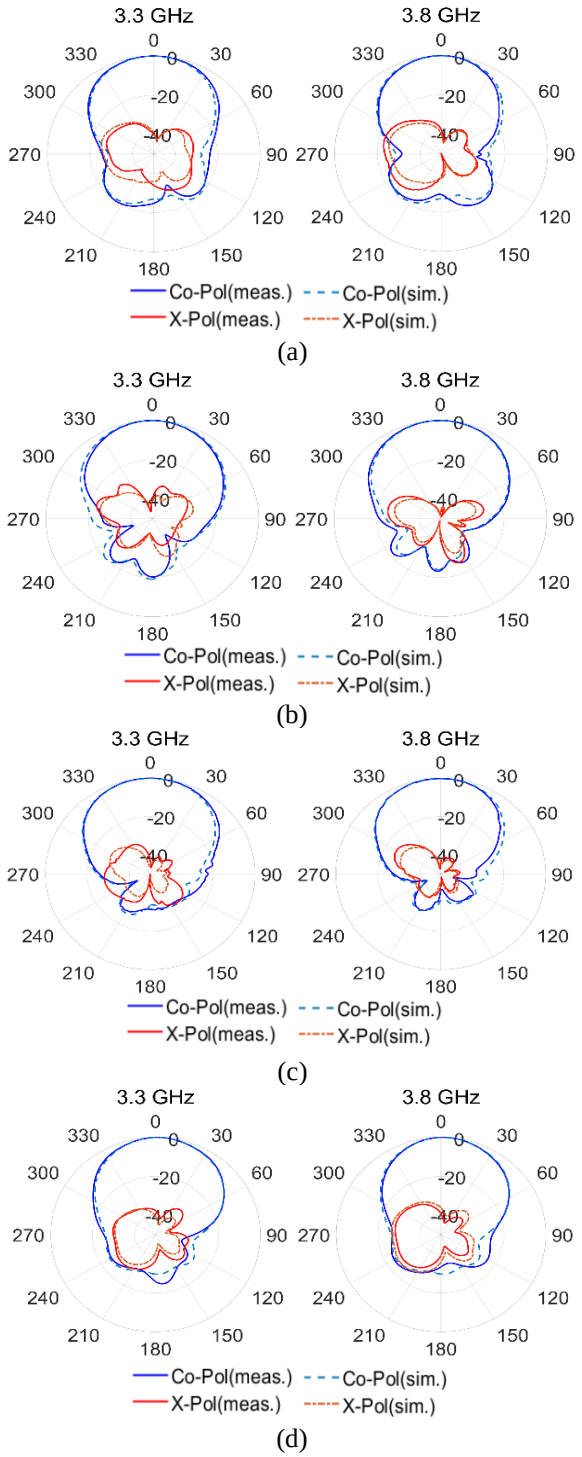

Fig. 12. Radiation patterns at 3.3 GHz and 3.8 GHz in (a) E-plane for port-1, (b) H-plane for port-1, (c) E-plane for port-2, and (d) H-plane for port-2.

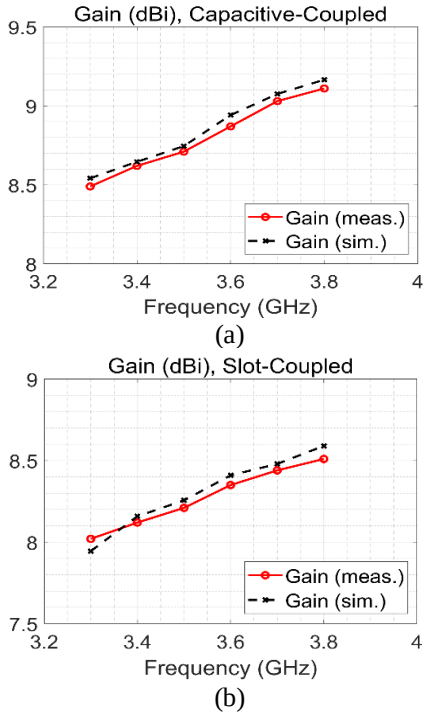

Fig. 13. Gain of the antenna (a) port-1 and (b) port-2.

V. CONCLUSION

In this study, a low-profile, wideband, hybrid-fed dual-polarized suspended stacked patch antenna with high isolation and high XPD has been introduced to be used in mMIMO arrays of sub-6 GHz 5G base stations (3.3-3.8 GHz). ±45° slant linear polarizations are established by using a slot-coupled feed and a capacitive-coupled probe feed. All performance specifications regarding wide IBW, good matching level, high isolation (< −47 dB), and high XPD (> 38 dB) have been obtained by a special design of stacked patches with hybrid feed excitations and making the coupling and interactions feeds and patches as low as possible. Measured patterns have symmetric, stable and broadside radiations with sufficient gains. Proposed antenna does not use any additional reflector plate to reduce back radiation. Hence, it is low-profile (10.6 mm) and has still good FBR (> 22 dB). In addition to desired high isolation and high XPD in 5G massive MIMO arrays, similar and stable characteristics (S-parameters, radiation patterns, gains) of each polarization port are necessary to have low ECC. Specifically, gain difference between each polarization port must be small (< 1 dB). In proposed design, this is achieved by gain difference of 0.5 dB, which is acceptable. Comparison of proposed work with similar ones in Table 1 also demonstrates superior and competitive features of the proposed antenna. As a result, it can be used as an antenna element in mMIMO array design in order to facilitate mMIMO array to reach its full performance.

ACKNOWLEDGMENT

This work is partially funded by The Scientific and Technological Research Council of Turkey (TUBITAK) under Grant No. 3180114.

REFERENCES

[1] P. K. Mishra, D. R. Jahagirda, and G. Kumar, "A review of broadband dual linearly polarized microstrip antenna designs with high isolation," *IEEE Antennas Propag. Mag.*, vol. 56, no. 6, pp. 238-251, Dec. 2014.

[2] Y. Luo, Q. X. Chu, and D. L. Wen, "A plus/minus 45-degree dual-polarized base-station antenna with enhanced cross-polarization discrimination via addition of four parasitic elements placed in a square contour," *IEEE Trans. Antennas Propag.*, vol. 64, no. 4, pp. 1514-1519, Apr. 2016.

[3] B. Feng, T. Luo, T. Zhou, and C.-Y.-D. Sim, "A dual-polarized antenna with low cross polarization, high gain, and isolation for the fifth-generation array multiple-input multiple-output communications," *Int. J. RF Microw. Comput. Aided Eng.*, May 2020, DOI: 10.1002/mmce.22278.

[4] X. T. Son, I. Park, and R. W. Ziolkowski, "Crossed dipoles antennas: A review," *IEEE Antennas Propag. Mag.*, vol. 15, no. 15, pp. 107-122, 2015.

[5] M. A. Jensen and J. W. Wallace, "A review of antennas and propagation for MIMO wireless communications," *IEEE Trans. Antennas Propag.*, vol. 52, no. 11, pp. 2810-2824, Nov. 2004.

[6] M. Li, X. Chen, A. Zhang, and K. A. Ahmed, "Dual-polarized broadband base station antenna backed with dielectric cavity for 5G communications," *IEEE Trans. Antennas Propag.*, vol. 18, no. 10, pp. 2051-2055, Oct. 2019.

[7] H.-W. Lai and K.-M. Luk, "Dual polarized patch antenna fed by meandering probes," *IEEE Trans. Antennas Propag.*, vol. 55, no. 9, pp. 2625-2627, Sept. 2007.

[8] F. Zhu, S. Gao, A. T. S. Ho, R. A. Abd-Alhameed, C. H. See, T. W. C. Brown, J. Li, and G. We, "Ultra-wideband dual-polarized patch antenna with four capacitively coupled feeds," *IEEE Trans. Antennas Propag.*, vol. 62, no. 5, pp. 2440-2449, May 2014.

[9] M. Ciydem and A. E. Miran, "Dual polarization wideband sub-6 GHz suspended patch antenna for 5G base stations," *IEEE Antennas Wirel. Propag. Lett.*, vol.19, no. 7, pp. 1142-1146, July 2020.

[10] M. Ciydem and S. Koc, "High isolation dual-polarized broadband antenna for base stations," *Microwave Opt. Technol. Lett.*, vol. 57, pp. 603-607, Jan. 2015.

[11] M. Barba, "A high-isolation, wideband and dual-linear polarization patch antenna," *IEEE Trans. Antennas Propag.*, vol. 56, no. 5, pp. 1472-1476, May 2008.

[12] A. A. Serra, P. Nepa, G. Manara, G. Tribellini, and S. Cioci, "A wideband dual-polarized stacked patch antenna," *IEEE Antennas Wirel. Propag. Lett.*, vol. 6, pp. 141-143, Apr. 2007.

[13] K.-L. Wong, H.-C. Tung, and T.-W. Chiou, "Broadband dual-polarized aperture-coupled patch antennas with modified H-shaped coupling slots," *IEEE Trans. Antennas Propag.*, vol. 50, no. 2, pp. 188-191, Aug. 2002.

[14] R. Caso, A. Serra, A. Buffi, M. R-Pino, P. Nepa, and G. Manara, "Dual-polarized slot-coupled patch antenna excited by a square ring slot," *IET Microw. Antennas Propag.*, vol. 5, no. 5, pp. 605-610, Apr. 2011.

[15] X. J. Lin, Z. M. Xie, and P. S. Zhang, "High isolation dual-polarized patch antenna with hybrid ring feeding," *Int. J. Antennas Propag.*, Article ID 6193102, 2017.

[16] L. H. Wen, S. Gao, Q. Luo, Q. Yang, W. Hu, and Y. Yin Y, "A low-cost differentially driven dual-polarized patch antenna by using open-loop resonators," *IEEE Trans. Antennas Propag.*, vol. 67, no. 4, pp. 2745-2750, Apr. 2019.

[17] K.-L. Wong and T.-W. Chiou, "Broadband dual-polarized patch antennas fed by capacitively coupled feed and slot-coupled feed," *IEEE Trans. Antennas Propag.*, vol. 50, no. 3, pp. 346-351, Mar. 2002.

[18] C. Sim, C. Chang, and J. Row, "Dual-feed dual-polarized patch antenna with low cross polarization and high isolation," *IEEE Trans. Antennas Propag.*, vol. 57, no. 10, pp. 3321-3324, Oct. 2009.

[19] K. Wei, Z. Zhang, W. Chen, and Z. Feng, "A novel hybrid-fed patch antenna with pattern diversity," *IEEE Antennas Wirel. Propag. Lett.*, vol. 9, pp. 562-565, 2010.

[20] T. An and W. Zhang, "A dual-polarized microstrip patch antenna using hybrid feed," *Electromagnetics*, vol. 30, pp. 256-268, 2010.

[21] J.-J. Xie, Y.-Z. Yin, J.-H. Wang, and X.-L. Liu, "Wideband dual-polarized electromagnetic fed patch antenna with high isolation and low cross-polarization," *IET Electron. Lett.*, vol. 49, no. 3, pp. 171-173, Jan. 2013.

[22] H. Saeidi-Manesh and G. Zhang, "High-isolation, low cross-polarization, dual-polarization, hybrid feed microstrip patch array antenna for MPAR application," *IEEE Trans. Antennas Propag.*, vol. 66, no. 5, pp. 2326-2332, May 2018.

[23] M. Xue, J. Liu, Z. Zhao, X. Yang, and Y. Yin, "Wideband dual-polarized hybrid fed patch antenna," *Int. J. RF Microw. Comput. Aided Eng.*, Mar. 2019, DOI: 10.1002/mmce.21711.

[24] J. Jiang, Y. Li, L. Zhao, and X. Liu, "Wideband MIMO directional antenna array with a simple meta-material decoupling structure for X-band applications," *Appl. Comput. Electromagn. Soc. J*, vol. 35, no. 5, pp.556-566, May 2020.

Mehmet Ciydem was born in 1971 in Ankara, Turkey. He received his B.Sc., M.Sc. and Ph.D. degrees all in Electrical Engineering from Middle East Technical University (METU), Ankara, Turkey with high honors. After working in defense industry (Aselsan, Havelsan, TAI) for many years, he founded Engitek Ltd. company in 2009 where he is President. He is an Associate Professor of electromagnetic theory and communications lecturing occasionally in several universities (Bilkent Univ., Gazi Univ., Karatay Univ., Hacettepe Univ., and Army War Academy). His research interests are in the areas of electromagnetics, wave propagation, antennas, RF/ microwave engineering, radar and communication systems.

Emre A. Miran was born in Izmir, Turkey in 1990. He received the B.S. degree in Electrical and Electronics Engineering from Dokuz Eylul University, Izmir, Turkey, in 2012. He is currently pursuing the Ph.D. degree in Electrical and Electronics Engineering Department at Middle East Technical University (METU), Ankara, Turkey. He was Teaching/Research Assistant at Micro/mm-wave Research Laboratory between 2012-2017. Then, he joined Engitek Ltd. as a Senior RF/Antenna Design Engineer. His research interest mainly includes the fields of electromagnetics, antenna design, RF system design, and radar imaging.